LONG-TERM ENVIRONMENTAL STABILITY OF HYDROTALCITE PRECIPITATED IN INDUSTRIAL SYSTEMS – A MOLECULAR MODELLING APPROACH

Chi L[1], Murthy V[1] and Smith HD[2]

1 – Charles Darwin University, Darwin, Northern Territory
2– APChem Scientific Consultants, Darwin, Northern Territory

Abstract

Hydrotalcite is a layered double hydroxide that precipitates spontaneously when seawater is used to neutralise wastewater from the Bayer process prior to disposal; however, ability to retain intercalated anions in the marine environment remains largely unstudied. This paper reports preliminary results obtained from novel computational molecular models being developed to examine hydrogen bonding and electrostatic forces within the molecular matrix of hydrotalcite; and give insight into its long-term environmental stability.

During in-situ precipitation, anionic species that may be harmful to or accumulate in biota become entrained in hydrotalcite via a number of bonding mechanisms, the most common of which is held to be intercalation. Modeling of intercalation suggests that a structured environment within the interlamellar space that hold anions principally by hydrogen bonding with either water molecules or terminal –OH groups of the Mg/Al lamellae forms. Electrostatic forces between anions and the metal hydroxide layers also exist, but the strength of these bonds is pH dependent and anion specific.

Results show that while the most of anions are strongly held by hydrotalcite, leaching and ion-exchange of less strongly bonded anions may still occur. This suggests that the long-term environmental stability of hydrotalcite may not be as great as previously thought. The models show potential as useful predictive tools for other hydrotalcite bonded anionic species not investigated here, although some refinements may be required to provide closer correlation with results measured for precipitates prepared under industrial conditions.

1. Introduction

Coastal alumina refineries often use seawater to neutralise their waste waters prior to disposal into the marine environment. This process takes advantage of the precipitation of synthetic hydrotalcites that are readily formed by reaction between magnesium salts and sodium aluminate solution and have variable stoichiometry. Hydrotalcites are layered double hydroxides (LDH) consisting of octahedral layers of mixed magnesium and aluminium hydroxides between which anionic compounds become intercalated. Their general stoichiometry is designated by:

$$[Mg_{1-x}Al_x(OH)_2]^{x+}[A^{n-}]_{x/y}.yH_2O$$

where A may be any anion.

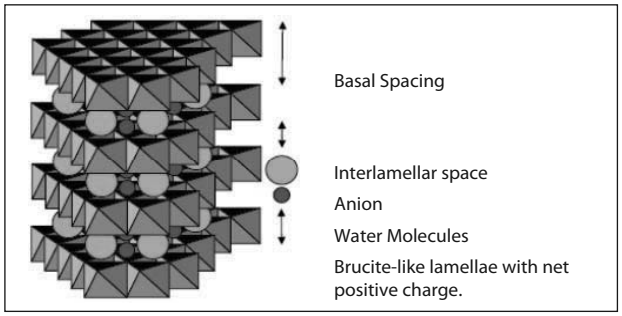

Figure 1: the layered double hydroxide structure as depicted in Goh et al (2008).

Industrial seawater neutralisation systems are dynamic, producing hydrotalcites dominated by materials having magnesium to aluminium ratios of 2:1 and 4:1 (Smith et al, 2005). CO_3^{2-} and $C_2O_4^{2-}$ are the most common intercalates, but any larger *in-situ* metalloid or transition metal molecule may be recovered. The efficiency of recovery is dependent upon changes to the molecular structure and charge density – both of which are affected by the pH at which precipitation occurs (Smith and Parkinson, 2006). Molecular structure, stoichiometry and the types of intercalate therefore depend upon industrial operating conditions under which the hydrotalcite is produced.

However, *in-situ* transition metal anions may be recovered from waste water in a number of ways, each of which exhibits a different degree of stability and ease by which the transition metal may be released back into the environment. The more environmentally stable precipitates are expected to form where transition metal anions replace Mg and/or Al in the octahedral layers. Those which are bonded as pillars joining the layers are likely to be less stable. Stability decreases further where the anions are intercalated or surface absorbed. The decreasing bond strengths makes them more susceptible to removal from the precipitate meaning that some precipitates may not be as stable as originally thought, and may create a source of future environmental contamination.

Intercalated anions contained within hydrotalcite found on the seafloor around coastal alumina refineries (e.g. CrO_4^{2-}) may be environmentally detrimental, so it is of interest to develop a means of estimating their stability within the hydrotalcite matrix and the rate at which they might be released. Modeling of the hydrotalcite structure offers an opportunity to do this and when compared with industrial operations, identify and select operating conditions that allow both the recovery of specific toxic anions and the stability of the hydrotalcite matrix to be maximized.

A number of experimental techniques (Prasanna and Vishu Kanath, 2008; Palmer et al, 2009) have been used to characterize hydrotalcite structures; but the disordering of hydrotalcite particles makes a full description of the arrangement of intercalated anions and water molecules within the interlamellar space difficult. Computational chemistry tools based on classical force fields and quantum-chemical methods are not limited in

this manner and therefore offer one means by which fundamental measures of molecular stability (such as bond strength) can be estimated. This in turn may provide opportunities to identify and select industrial operating conditions that permit both the recovery of specific anions from solution and the stability of the hydrotalcite matrix to be maximized.

Over the past decade, a number of molecular models leading to improved insight of hydrotalcite's interlamellar structure and dynamics (Aicken et al, 1997; Fogg et al, 1999; Rives and Angeles Ulibarri, 1999; Wang et al, 2003; Zhang et al, 2008; Kovar et al, 2007) have been reported. These include descriptions of hydration and swelling (Smith, 1998; Kumar et al, 2006) ENREF_14, bonding (Wang et al, 2005; Kumar et al, 2007) and diffusivity of intercalated anions (Newman et al, 2002). These models are generally restricted to simple species such as Cl-, CO32- and NO3- or complicated organics, with intercalated transition metal anions generally unreported. This paper reports preliminary outcomes of a project that seeks to address this knowledge gap by comparing computational molecular dynamics simulations for hydrotalcites containing transition metal anions against those for hydrotalcite intercalated with CO32-.

2. Method

2.1 Preparation of synthetic hydrotalcite

Batch solutions of 1 molar sodium aluminate were prepared by dissolution of aluminium pellets or foil in sodium hydroxide. These solutions were cooled and filtered to remove any residue prior to final dilution and standardization. Synthetic hydrotalcites of varying stoichiometry were prepared by mixing varying volumes of sodium aluminate and 1 molar magnesium chloride. Where required, sodium salts of vanadate, chromate, and carbonate were dissolved and added directly into the sodium aluminate immediately prior to reaction. The amounts of these salts were calculated to produce solution concentrations representative of the industrial process.

To provide an insight into intercalate stability, the hydrotalcite was washed first with water and then with a strong ion-exchange solution (e.g. 2.5M Na2CO3). 0.3g portions of hydrotalcite were washed with 40mls demineralised water to remove surface adsorbed anions. Other 0.3g portions were stirred with 10ml 2.5M Na2CO3 for a minimum 30 minutes followed by addition of 30ml demineralised water to remove ion-exchangeable anions. Each solution was then allowed to stand for a minimum 24hours, prior to filtration and drying in air. All filtrates were then mixed with 2ml of 70% HNO3 and diluted to 50ml with demineralised water prior to submission for ICP-MS analysis. The air dried samples were analysed by Powder X-Ray diffraction.

XRD patterns were obtained using Co Kα (1.789Å) radiation on a Philips PW3710 coupled with a 1050 Goniometer and using curved graphite PW1752 diffracted beam monochromator with receiving slit height of 0.2 mm. Diffraction patterns were recorded at 10kV/10mA across the range 5 to 70 degrees 2θ, using a step size of 0.020 degrees timed at 1 second per step. Where diffraction patterns were poor, the 2θ step size was reduced and a longer analytical time used to provide greater sensitivity. Peaks were defined using calculations based on determination of the minimum of the second derivative with minimum significance of 0.6 degrees 2θ.

2.2 Computational Modeling

The initial crystal structure was based on the previously reported crystal structure of Mg4Al2(OH)12 CO3 .3H2O. The basic model was developed using average results from XRD analyses. Using the measured lattice parameters a and b = 3.054Å; c = 22.809Å; a = 90°; b = 90°; and g = 120°, models of 2 hydrotalcite layers, each containing 8 by 6 atomic rows and giving total parameters a = 24.432 Å, b = 18.324Å, and c = 22.809Å were constructed (refer Figure 2). The unit cell of the crystal was assumed to be contained within the triclinic Bravais Lattice having space group R-3m.

Mg and Al atoms were randomly distributed within the structural matrix to generate a structure having a Mg/Al ratio of 2:1 with each hydroxide layer containing a total layer charge of +8, which was balanced by the random introduction of anions between two host layers. A similar 4:1 supercell was also built.

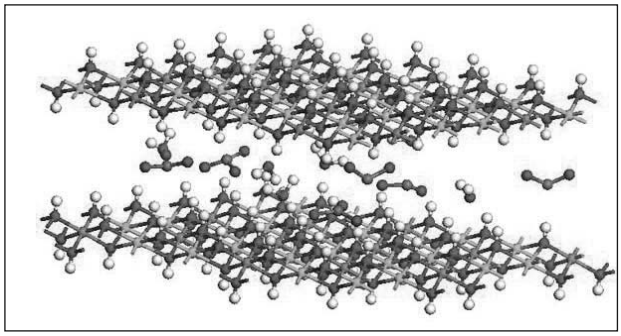

Figure2: Hydrotalcite supercell containing interlamellar water molecules. Green balls represent Mg atoms, pink = Al, red= oxygen, and grey=hydrogen.

Molecular dynamic simulations were then performed using Forcite in Material Studio (4.4 and 5.5). Universal Forcefield parameters were assigned to all atoms in the LDH, the water, and the anions permitting generalized geometry optimizations and MD simulations to be undertaken. Charges for the LDH and water molecules were modified according to the CLAYFF force field (Cygan et al, 2004; Cygan et al, 2009) to compensate for influences of layer charge on interlamellar anion packing modes.

Prior to MD simulations geometry optimizations of the hydrotalcite intercalated with anions and water molecules were carried out. Electrostatic and van der Waals energies were calculated by the Ewald summation method and minimizations carried out by Quasi-Newton procedure. Periodic boundary conditions were applied in three dimensions so that the simulation cell is effectively repeated infinitely in each direction.

Initially the host layers in the supercell were held as rigid units to allow the lattice parameter c (gallery height) to vary. The structures of the anions were also held rigid using the 'keep motion groups rigid' function available in geometry optimization in Forcite. This enabled the mutual positions of the host layers and positions and orientations of the guest layers (anions and water molecules) to vary and optimize to a minimum with respect to each other.

These optimized structures were then used as the starting configurations for the MD simulations, performed in the NVT-ensemble (constant-volume/constant-temperature) where atoms in both the host and guest layers were released. Since all atoms in each system were completely free to move during these simulations, using the constant-volume modelling approach with a fixed cell shape does not introduce significant limitations to the resulting interfacial structure, dynamics and energetics of water.

MD simulations were performed in NVT-ensemble at 300 K and a time step of 0.001ps was used for all simulations. Analysis of the simulations revealed that equilibrium values for the thermodynamic parameters were generally reached within the first 20 ps using an Andersen thermostat. An initial MD simulation of 30ps was carried out using Andersen thermostat followed by 200ps simulations with Nosé thermostat for different hydration states, n, of the system.

3. Results

Lattice parameters determined from powder X-ray diffraction measurements made for synthetic hydrotalcites are presented in Table 1. They reflect the distinction between the two major hydrotalcite phases and are consistent with generally accepted values published elsewhere.

Data presented in Table 2 indicates that the ability of synthetic hydrotalcite to recover and retain transition metal anions varies across anion type and pH. Although these data are statistically weak, it can be generally concluded that a large proportion of transition metal anions retained by hydrotalcite are not easily removed by washing or CO32- ion-exchange.

The relative ease by which anions can move within the interlamellar space is estimated from self-diffusion coefficients determined from molecular models and presented in Table 3. Variability of parameters across anion and hydrotalcite type provides insight into structural stability. The effects of interlamellar swelling, which can also impact anion mobility is shown by varying the number of water molecules resident within the interlamellar space and presented in Table 4.

Table 1: Experimental lattice parameters determined from PXRD analyses of synthetic hydrotalcites.

Parameter	$[Mg_{0.67}Al_{0.33}(OH)_2](CO_3)_{0.16}.xH_2O$	$[Mg_{0.80}Al_{0.20}(OH)_2](CO_3)_{0.10}Cl_{0.20}.xH_2O$
x	0.33	0.20
a	3.12	3.15
c	22.8	24.3
l	2.8	3.3
t_a	242.1	112.3
t_c	173.8	195.2
d_{003}	7.61	8.11
d_{110}	1.56	1.57

Where *a*, *c*, *l* (interlamellar space); t_a and t_c as the crystallite thickness along the *a* and *c* planes respectively, are expressed as angstroms (Å). *x* is the ratio of trivalent:total cations ($A/(A+M)$) in the lamellar structure

Table 2: Relative proportions of *in-situ* anions recovered during precipitation of hydrotalcite and then released by water washing and ion-exchange.

A: $[Mg_{0.67}Al_{0.33}(OH)_2](CO_3)_{0.16}.xH_2O$					
Anion	**n**	**Recovered from solution**	**Removed by water**	**Removed by carbonate**	**Not removed**
VO_4^{3-}	2	46.4 %	4.5 %	14.0 %	27.9%
CrO_4^{2-}	5	85.7 ± 4.2%	3.2 %	11.0 %	71.4 %
B: $[Mg_{0.80}Al_{0.20}(OH)_2](CO_3)_{0.10}Cl_{0.20}.xH_2O$					
Anion	***n***	***Recovered from solution***	**Removed by water**	**Removed by carbonate**	**Not removed**
VO_4^{3-}	2	78.4 %	0.4 %	5.8 %	72.2 %
CrO_4^{2-}	6	99.4 ± 0.1%	14.2 %	27.8 %	57.4 %
MoO_4^{2-}	6	60.9 ± 9.5 %	2.3 %	28.9 %	29.7 %
MnO_4^{-}	1	0.2 %	0.1%	< 0.1%	< 0.1%

Table 3: Modelled self diffusion coefficients (expressed as Å²/ps) for anions trapped within the interlamellar space of industrial hydrotalcites.

Intercalate	$[Mg_{0.67}Al_{0.33}(OH)_2](CO_3)_{0.16}.xH_2O$	$[Mg_{0.80}Al_{0.20}(OH)_2](CO_3)_{0.10}Cl_{0.20}.xH_2O$
CO_3^{2-}	1.07×10^{-3}	
$C_2O_4^{2-}$	6.26×10^{-4}	
CrO_4^{2-}	2.19×10^{-3}	4.14×10^{-3}
MoO_4^{2-}	4.01×10^{-3}	2.22×10^{-3}
VO_4^{3-}	2.67×10^{-3}	

Table 4: Variation in interlamellar space (expressed as Å) with increasing levels of water placed into the interlamellar space of $[Mg_{0.67}Al_{0.33}(OH)_2](CO_3)_{0.16}.xH_2O$.

Number of molecules of H_2O	0	4	12	18
Intercalate				
CO_3^{2-}	2.53	2.86		
$C_2O_4^{2-}$	2.53	3.13		
CrO_4^{2-}	3.61	3.87	4.16	4.19
MoO_4^{2-}	3.57	3.80		
VO_4^{3-}	2.54	3.10		

4. Discussion

Charge density calculations can be used to estimate the relative stabilities of different anion types contained within the hydrotalcite matrix. The first step in is to determine the efficiency of the anion recovery process. This is dependent upon pH and a number of physical factors including the anion's dimensions, charge density and its ability to successfully compete with other anions for bonding at the hydrotalcite lamellae where substitution of Mg^{2+} by Al^{3+} has created a net positive charge. A measure of the efficiency of anion recovery by hydrotalcite (E_R), can be estimated according to:

$$E_R = \left(\frac{[A^{x-}]}{[A^{3+}]} \right) / \frac{Q_{HT}}{Q_A} \qquad (1)$$

where A^{x-} is the anion and charge densities are represented by *Q*. Calculation of individual charge densities of the hydrotalcite lamella (Q_{HT}) and the interlamellar anions (Q_A) are discussed below.

Average lamella charge density and the average distance between adjacent interlamellar anions can be calculated directly from measured stoichiometry and PXRD data. The average distance between adjacent interlamellar anions (d_z) may be determined from:

$$d_z = \frac{a\sqrt{n}}{x} \qquad (2)$$

where *x* is the mole fraction of Al^{3+}, *n* is the anionic charge and *a* is the average lamellar cation – cation distance (nm), calculated from the measured d_{110} spacing. This calculation also permits the point locations to be estimated and applied to molecular models.

Where the bonding angle (θ) between cations is known, charge density across the surface of the lamella may be calculated using:.

$$Q_{HT} = \frac{2e}{(a^2 \sin\theta)} \qquad (3)$$

This provides a 'two-dimensional' measure (expressed as e/nm²) which is suitable for layers (Ni et al, 2006). However, anions

require a measure of charge density over three dimensions (e/nm^3) so a more meaningful concept requires the dissipation of charge density into the interlamellar space (*l*) to be taken into account by adjusting equation 3 to:

$$Q_{HT} = \frac{R}{1/2 * I(a^2 \sin\theta)} \quad (4)$$

The presence of transition metal anions in hydrotalcites does not appreciably affect d_{110}, so any impact on Q_{HT} through changes to either *a* or *l* remains negligible. As more Al^{3+} enters into the lamellar structure charge density increases, but remains generally independent of the type of intercalate present during precipitation. Conversely, interpillar distances vary significantly with the type and amount of transition metal present, resulting in increase to d_z values with larger anion dimensions.

The next step is to consider charge density of the anions. For single molecules of volume *V*, anion charge density per unit volume can be calculated using:

$$Q_A = \frac{n}{V_{ionic}} \quad (5)$$

where *V* is the ionic volume obtained from literature (Jenkins et al, 1999; Roobottom et al; 1999). From these anion charge densities and the maximum number of anions required to balance a single charge point on each hydrotalcite lamella can be calculated using:

$$N_{HT} = \frac{Q_c}{Q_a} \quad (6)$$

E_R is then determined by comparison with values determined from experimental measurements of the anion:Al molar ratio ($N_{HT\ Exp}$) for the solids using the previously defined equation:

$$E_R = \left(\frac{[A^{x-}]}{[A^{3+}]}\right) / \frac{Q_{HT}}{Q_A} \quad (7)$$

These values are presented in Table 5. They suggest that recovery and possibly the stability of anions retained within the interlamellar space of $[Mg_{0.67}Al_{0.33}(OH)_2](CO_3)_{0.16}.xH_2O$ follow a sequence: $CO_3^{2-} > VO_4^{3-} > MoO_4^{2-} > CrO_4^{2-}$. For $[Mg_{0.80}Al0_{0.20}(OH)_2](CO_3)_{0.10}Cl_{0.20}.xH_2O$, the sequence is: $VO_4^{3-} > MoO_4^{2-} > CrO_4^{2-} > CO_3^{2-}$. However, recovery of CrO_4^{2-}, MnO_4^- and MoO_4^{2-} is lower than expected and the recovery sequence does not appear to compare closely with experimentally acquired data (refer Table 2). Further work is required to determine if this is a function of competition between anions for bonding locations. While they may still undergo a degree of adsorption and/or intercalation, it is possible that they do not participate in charge dissipation in this manner because they are otherwise bonded to the hydrotalcite lamellae.

Table 5: Charge density, predicted and experimentally determined maximum charge balance ratios (N_{Exp}) for some transition metal anions and carbonate.

	Q_a	$N_{2:1\ HT}$	$N_{2:1\ HT\ Exp}$	E_R	$N_{4:1\ HT}$	$N_{4:1\ HT\ Exp}$	E_R
2:1 LDH	8.38						
4:1 LDH	12.42						
VO_4^{3-}	42.9	0.20	0.05	25%	0.29	0.25	86%
CO_3^{2-}	32.8	0.26	0.23	88%	0.38	0.04	11%
CrO_4^{2-}	25.0	0.34	0.04	12%	0.50	0.13	26%
MoO_4^{2-}	22.7	0.37	0.03	8%	0.55	0.20	36%
MnO_4^-	11.4	0.74	<0.01	<1%	1.09	0.01	1%

5. Computational modelling

Computational modelling provides another range of parameters that can be used to describe the stability of anions within the molecular matrix. Self-diffusion is one concept that can be used to evaluate the mobility of anions within the interlayer space and provide insight into long-term stability. The diffusion co-efficient (*D*) is determined from the modelled velocity autocorrelation function using:

$$D = \lim_{t\to\infty} \frac{1}{6t} \left\langle \left| r(t) - r(0) \right|^2 \right\rangle \quad (8)$$

In practice, it is calculated from the gradient of the longest part of the flattest sequence of the mean-square displacement (MSD) graph (Zhang et al, 2008), as shown in Figure 3. It is a measure of the average planar distance of all random movements of the anions in the interlamellar space and is therefore analogous to Brownian motion. MSD is proportional to the strength of the electrostatic bonds between the anion and the hydroxide functional groups of the layer and relates directly to the relative ease with which an anion can be removed from the interlayer space by ion-exchange mechanisms.

Figure 3 show a gradual increase along an almost constant gradient that terminates with a significant upward curvature. Gradients are measured over the 50 – 350ps span where the graph remained essentially constant. The flatness of MSD lines for $C_2O_4^{2-}$, CO_3^{2-} and VO_4^{3-} indicate that these anions are likely to be tightly held by electrostatic forces within the interlamellar space. CrO_4^{2-} and MoO_4^{2-} show significant curvature, suggesting weaker bonding and a greater degree of mobility within the interlamellar space.

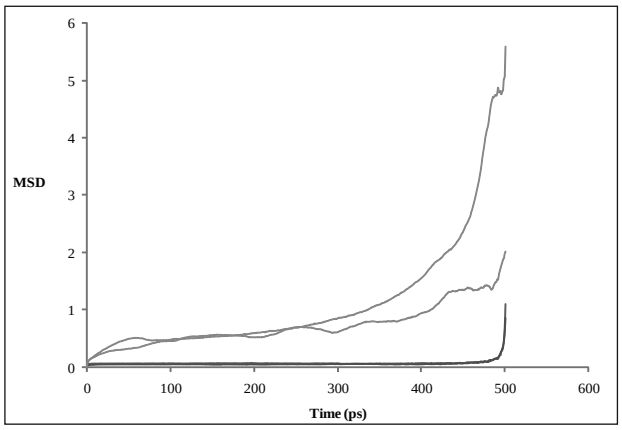

Figure 3: relative diffusivity of anions in $[Mg_{0.67}Al_{0.33}(OH)_2](CO_3)_{0.16}.xH_2O$.

Values for diffusivity of anions estimated from the models were calculated indicate that bond stability of anions contained by $[Mg_{0.67}Al_{0.33}(OH)_2](CO_3)_{0.16}.xH_2O$ follows the sequence $VO_4^{3-} > CO_3^{2-} > C_2O_4^{2-} > MoO_4^{2-} > CrO_4^{2-}$. This compares well with the sequence obtained using charge density calculations but again, not for the experimentally measured data obtained from desorption studies.

It appears that calculated diffusion rates across the interlamellar space tend towards higher values for $[Mg_{0.80}Al0_{0.20}(OH)_2](CO_3)_{0.10}Cl_{0.20}.xH_2O$ than $[Mg_{0.67}Al_{0.33}(OH)_2](CO_3)_{0.16}.xH_2O$ – which reflects the greater distance between the Al points of charge. While the total volume of electrostatic charge generated in the $[Mg_{0.80}Al0_{0.20}(OH)_2](CO_3)_{0.10}Cl_{0.20}.xH_2O$ interlamellar space remains comparable to that of $[Mg_{0.67}Al_{0.33}(OH)_2](CO_3)_{0.16}.xH_2O$, the decreased availability of CO_3^{2-} in solution should reduce competition and allow more highly charged molecules to move into the interlamellar space. However, the increased rates of diffusion also mean that transition metal anions may be more readily removed from the interlamellar space.

Preliminary modelling also suggests that the amount of interlamellar water may have an important impact upon the mobility of anions within the interlamellar space. Where water exists in a layer between the anion and the terminal hydroxyl groups of hydrotalcite, outer-sphere surface complexation results in the anion becoming more mobile (Kalinichev et al, 2000). However, further detailed modelling is required to determine if the presence of additional interlamellar water affects the rates of diffusion and the comparative increase in diffusion for all anions in the low pH hydrotalcite.

This may be of serious concern as CrO_4^{2-} is a potentially toxic species that becomes trapped within the interlamellar space. Its position at the lower end of the sequence suggests that it may undergo ion-exchange and be released back into the environment from industrial precipitates. The rate of exchange will be dependent upon the degree of swelling, the strength of the bonds and the nature of the ion-exchange agent, which in the marine environment is most likely to be SO_4^{2-} and Cl^-.

These species have not been included in the models thus far, so it would be of great interest to see where they would fit in the sequence particularly as this might provide better insight into the suitability of hydrotalcite as long-term ameliorant for CrO_4^{2-}. If they hold a position of greater stability in the sequence, then it is reasonable to conclude that they are likely to dislodge CrO_4^{2-} from the interlamellar space.

6. Conclusions

Basic computational molecular models describing the two most common types of hydrotalcite precipitated in the industrial seawater neutralisation systems have been developed. The preliminary results provided here suggest that they have a role to play in describing the stability of anions that have been recovered by hydrotalcite during seawater neutralisation of Bayer process waste waters.

They provide outcomes comparable with those obtained from charge density calculations using experimental X-ray diffraction data and demonstrate the ability to compensate for structural change brought about by factors such as interlamellar swelling. Using measures of self-diffusion, the stability of anions within the interlamellar space was shown to follow a sequence: $VO_4^{3-} > CO_3^{2-} > C_2O_4^{2-} > MoO_4^{2-} > CrO_4^{2-}$.

However, there is a need to produce a more detailed sequence of interlamellar stability that covers a wider range of anions so that the long term environmental effects of hydrotalcite in the marine environment can be better modelled.

The basic models have produced meaningful outcomes, but further work is required before they can be applied with confidence to other ionic species. Some next steps include constructing larger unit cell structures and measuring other parameters such as hydration energies to identify preferred hydration states and determine points where the molecules are the most stable in order to produce more accurate models.

Alternate forcefields such as the *ab initio* forcefield COMPASS and optimization of anion structure and charges using the B3LYP (Becke, 1988; Becke 1993) method and the LANL2DZ_ENREF_23 (Wadt and Hay, 1995) basis set, suitable for transition metals_ENREF_24 (Hedegard et al, 2009) are to be investigated. These should lead to better definitions of competition for bonding sites, the locations of anions within the molecular structure, and of the influence of interlamellar water on the rate of their diffusion. Once completed, a better indication of the environmental stability of industrial hydrotalcites in the marine environment may be possible.

References

Aicken, AM, Bell IS, Coveny PV & Jones W (1997), 'Simulation of layered double hydroxide intercalates', *J. Advanced Materials,* vol. 9, no.6, pp. 496-500.

Becke, AD (1988), 'Correlation energy of an inhomogeneous electron gas: A coordinate-space model', *The Journal of Chemical Physics*, vol. 88, no.2, pp.1053-1062.

Becke, AD (1993) 'Density-Functional Thermochemistry .3. the Role of Exact Exchange', *The Journal of Chemical Physics*, vol. 98, no.7, pp. 5648-5652.

Cygan RT, Greathouse JA, Heinz H & Kalinichev AG (2009), 'Molecular models and simulations of layered materials', *Journal of Materials Chemistry,* vol. 19, pp. 2470-2481.

Cygan, RT, Liang, J-J. & Kalinichev AG (2004), 'Molecular Models of Hydroxide, Oxyhydroxide, and Clay Phases and the Development of a General Force Field', *The Journal of Physical Chemistry B*, vol. *108*, no. 4, pp. 1255-1266.

Fogg, AM, Rohl AL, Parkinson GM & O'Hare D. (1999), 'Predicting Guest Orientations in Layered Double Hydroxide Intercalates', *Chemistry of Materials, vol. 11*, pp. 1194-1200.

Goh KH, Lim TT and Dong Z (2008), 'Application of layered double hydroxides for removal of oxyanions: A review', *Water Research,* vol. 42, no. 6-7, pp. 1343-1368.

Hedegård, ED, Bendix J & Sauer, SPA (2009), 'Partial Charges as Reactivity Descriptors for Nitrido Complexes', *Journal of Molecular Structure: THEOCHEM*, vol. 913, pp. 1-7.

Jenkins HDB, Roobottom HK, Passmore J & Glasser L (1999), 'Relationships among Ionic Lattice Energies, Molecular (Formula Unit) Volumes, and Thermochemical Radii', *Inorganic Chemistry*, vol. 38, no. 16, pp. 3609-3620.

Kalinichev AG, Wang J and James-Kirkpatrik R (2000), 'Molecular dynamics simulation of layered double hydroxides', *AIChe Symposium Series,* vol. 325, pp. 221-225.

Kovář P, Pospíšil M, Nocchetti M, Čapková P & Melánová, K (2007), 'Molecular modeling of layered double hydroxide intercalated with benzoate, modeling and experiment', *Journal of Molecular Modeling*, vol. *13*, no. 8, pp. 937-942.

Kumar PP, Kalinichev AG & Kirkpatrick RJ (2007), 'Molecular Dynamics Simulation of the Energetics and Structure of Layered Double Hydroxides Intercalated with Carboxylic Acids', *The Journal of Physical Chemistry C,* vol. 111, no. 36, pp. 13517-13523.

Newman SP, Di Cristina T, Coveney PV & Jones W,(2002), Molecular Dynamics Simulation of Cationic and Anionic Clays Containing Amino Acids', *Langmuir*, vol. 18, pp. 2933-2939.

Ni Z, Pan G, Wang L, Yu W, Fang C and Li D (2006), 'Structure and properties of hydrotalcite using electrostatic potential energy model' *Chinese Journal of Chemical Physics,* vol. 1, no. 3, pp. 278-281.

Padma-Kumar, PP, Kalinichev, AG & Kirkpatrick, RJ (2006) 'Hydration, Swelling, Interlayer Structure, and Hydrogen Bonding in Organolayered Double Hydroxides: Insights from Molecular Dynamics Simulation of Citrate-Intercalated Hydrotalcite', *The Journal of Physical Chemistry B, vol. 110*, no. 9, pp. 3841-3844.

Palmer, SJ, Frost, RL & Nguyen, T (2009), 'Hydrotalcites and their role in coordination of anions in Bayer liquors: Anion binding in layered double hydroxides', *Coordination Chemistry Reviews*, vol. *253*, no. 1-2, pp. 250-267.

Prasanna, SV & Vishnu Kamath, P (2008), 'Chromate uptake characteristics of the pristine layered double hydroxides of Mg with Al', *Solid State Sciences*, vol. *10*, no. 3, pp. 260-266.

Rives V & Angeles-Ulibarri M (1999), 'Layered double hydroxides (LDH) intercalated with metal coordination compounds and oxometalates', *Coordination Chemistry Reviews,* vol. 181, no. 1, pp. 61-120.

Roobottom HK, Jenkins HDB, Passmore J & Glasser L (1999), 'Thermochemical Radii of Complex Ions', *Journal of Chemical Education,* vol. 76, no. 11, pp. 1570-1573.

Smith, DE (1998), 'Molecular Computer Simulations of the Swelling Properties and Interlayer Structure of Cesium Montmorillonite', *Langmuir*, vol. 14, no. 20, p. 5959-5967.

Smith HD, Hart RD & Parkinson GM (2005), 'In situ absorption of molybdate and vanadate during precipitation of hydrotalcite from sodium aluminate solutions', *Journal of Crystal Growth*, vol. 275, pp. e1665-e1671.

Smith HD & Parkinson GM (2005), 'Seawater Neutralisation: Factors affecting adsorption of anionic chemical species', *Proceedings of the 7th international Alumina quality workshop,* November 2005, Perth, Western Australia, pp. 221-224.

Tomasi, J, Mennucci, B & Cancès, E (1999), 'The IEF version of the PCM solvation method: An overview of a new method addressed to study molecular solutes at the QM ab initio level', *Journal of Molecular Structure: THEOCHEM*, vol. 464, pp. 211-226.

Wadt, WR & Hay, PJ. (1985), '*Ab initio* effective core potentials for molecular calculations. Potentials for main group elements Na to Bi', *The Journal of Chemical Physics*, vol. *82*, no.1 , pp. 284-298.

Wang J, Kalinichev AG, Amonette JE & James-Kirkpatrick R (2003), 'Interlayer structure and dynamics of Cl-bearing hydrotalcite: far infrared spectroscopy and molecular dynamics modelling', *American Mineralogist*, vol. 88, pp. 398-409.

Wang, J, Kalinichev, AG, Kirkpatrick, RJ & Cygan RT (2005), 'Structure, energetics, and dynamics of water adsorbed on the muscovite (001) surface: a molecular dynamics simulation', *Journal of Physical Chemistry B,* vol. 109, pp. 15893-15905.

Zhang H, Xu Z, Lu GQ & Smith SC (2008), 'Intercalation of sulfonate into layered double hydroxide: Comparison of simulation with experiment', *The Journal of Physical Chemistry C*, vol.113, no. 2, pp. 559-566.